AD-A069 159 HARRY DIAMOND LABS ADELPHI MD F/G 20/13
AN INITIAL MODEL FOR THE FINITE DISPLACEMENT RESPONSE CHARACTER--ETC(U)
FEB 79 T M DRZEWIECKI
UNCLASSIFIED HDL-TR-1868 NL

1 OF 1
AD A069159

END
DATE FILMED
7-79
DDC

HDL-TR-1868
February 1979

An Initial Model for the Finite Displacement Response Characteristics of a Fluidyne Pump

Tadeusz M. Drzewiecki

U.S. Army Electronics Research and Development Command
Harry Diamond Laboratories
Adelphi, MD 20783

UNCLASSIFIED

SECURITY CLASSIFICATION OF THIS PAGE (When Data Entered)

REPORT DOCUMENTATION PAGE	READ INSTRUCTIONS BEFORE COMPLETING FORM
1. REPORT NUMBER: HDL-TR-1868	2. GOVT ACCESSION NO. / 3. RECIPIENT'S CATALOG NUMBER
4. TITLE (and Subtitle): An Initial Model for the Finite Displacement Response Characteristics of a Fluidyne Pump	5. TYPE OF REPORT & PERIOD COVERED: Technical Report
	6. PERFORMING ORG. REPORT NUMBER
7. AUTHOR(s): Tadeusz M. Drzewiecki	8. CONTRACT OR GRANT NUMBER(s): DA: 1T161101A91A
9. PERFORMING ORGANIZATION NAME AND ADDRESS: Harry Diamond Laboratories, 2800 Powder Mill Road, Adelphi, MD 20783	10. PROGRAM ELEMENT, PROJECT, TASK AREA & WORK UNIT NUMBERS: Program Ele: 6.11.01.A
11. CONTROLLING OFFICE NAME AND ADDRESS: U.S. Army Materiel Development and Readiness Command, Alexandria, VA 22333	12. REPORT DATE: February 1979 13. NUMBER OF PAGES: 45
14. MONITORING AGENCY NAME & ADDRESS (if different from Controlling Office): 43 p.	15. SECURITY CLASS. (of this report): Unclassified 15a. DECLASSIFICATION/DOWNGRADING SCHEDULE

16. DISTRIBUTION STATEMENT (of this Report)

Approved for public release; distribution unlimited

17. DISTRIBUTION STATEMENT (of the abstract entered in Block 20, if different from Report)

18. SUPPLEMENTARY NOTES

HDL Project: A107C4
DRCMS Code: 61110191A.0011

19. KEY WORDS (Continue on reverse side if necessary and identify by block number)

Pump	Thermodynamics
Fluidyne	Fluidics

20. ABSTRACT (Continue on reverse side if necessary and identify by block number)

This paper is the final report on the independent laboratory in-house research (ILIR) sponsored work by the Harry Diamond Laboratories on the Fluidyne pump. The effort started with a survey of the extant literature on the subject, continued with experimental observations that led to a mathematical model, and has culminated with a comprehensive statement on the physical operation of the pump. →

DD FORM 1 JAN 73 1473 EDITION OF 1 NOV 65 IS OBSOLETE

UNCLASSIFIED

SECURITY CLASSIFICATION OF THIS PAGE (When Data Entered)

163 050

The literature is particularly sparse on the subject; hence, only the basic references are cited. The report presents a detailed mathematical model of the fluid mechanical and thermodynamic processes occurring during oscillation. A positive-feedback simulation model is postulated that demonstrates, for the first time, physically why there is an onset of oscillations and subsequent sustained motion. This model is based on actual observations of the startup process in a prototype pump.

The initially reported thermodynamic efficiency of this heat engine was less than 0.3 percent. Currently, Fluidyne pumps have demonstrated efficiencies of about 2 percent. The peak efficiencies, however, may theoretically approach 10 percent. The mathematical model has shown that large losses occur in the heat transfer to the working gas, heat lossses to the displacer liquid, and friction in the output line. Improvements in these areas may dramatically improve the observed overall efficiency. The efficiency of the cycle itself, that is, the work done by the thermodynamic cycle relative to the output work, is on the order of 10 percent. Finally, the cycle is shown to be close to a Carnot cycle as opposed to the originally supposed Stirling cycle. This last observation has considerable and significant ramifications as far as future analysis is concerned.

CONTENTS

APPENDICES

FIGURES

1. INTRODUCTION

The introduction of the Fluidyne "no-moving-parts" pump in 1971[1,2] stimulated some new interest in the conversion of low grade, low temperature heat energy into useful work. The basic principle was reported to be a closed Stirling cycle, wherein two adjacent U-tubes of liquid were stimulated into oscillation by the application of heat to a connecting U-tube of gas. The open U-tube of oscillating liquid thus was the source of power to do work. A linearized lossless model was proposed by Elrod[3] that predicted the onset of oscillation and the frequency thereof. No satisfactory physical explanation was offered for the phenomenon, however.

With the coming of the energy crisis, initial studies on reclaiming waste heat were proposed by the Harry Diamond Laboratories using the Fluidyne. With the proposed increased dependence on nuclear power, additional interest in the Fluidyne became apparent when it was conceptually demonstrated that a Fluidyne could serve as an independent power source for fluidic monitoring and control schemes that are completely decoupled from standard electromechanical systems in use. Such incidents as the Brown's Ferry fire and the loss of secondary controls could be avoided by using the residual nuclear heat to operate a self-contained Fluidyne pump and fluidic sensors and controls operating within the pressure vessel itself. A system having no moving parts except the working fluid would be extremely reliable.

The poor efficiency of currently available[3] pumps allows profitable operation only where the heat source costs are negligible or, as in a nuclear plant, not of concern. Improvement of the efficiency would allow greater utilization and would decrease the unit size per unit output power. This decrease would allow the use of smaller devices in such applications as nuclear power plant auxiliary control systems.

This report presents a comprehensive basis for the understanding of the Fluidyne pump's operation, analyzes the concept of the efficiency of the thermodynamic cycle, and provides important guidelines for design.

2. PHYSICAL DESCRIPTION OF FLUIDYNE STARTUP

In the schematic diagram (fig. 1), a reservoir of liquid is shown with a U-tube of gas connecting two liquid columns. A separate U-tube filled with the liquid is situated with one end directly beneath one end of the gas-filled tube. The other end, for this analysis, is left open to the atmosphere. The free surface motion indicates the output mechanical work available.

The gas volume may be thought to be composed of two imaginary halves. The right half, labeled "2," which connects to the output tube, is the hot side; the left half, labeled "1," is the cold side. Heat is continually applied to the right half, and the left side is maintained at a lower or ambient temperature. In the experiments conducted, the cold side was cooled by natural convection to ambient.

---

[1] *C. West, The Fluidyne Heat Engine, United Kingdom Atomic Energy Authority, Harwell, UK, AERE-R-6775 (1971).*

[2] *C. West, And Yet It Moves, New Scientist, 29 (August 1974).*

[3] *H. Elrod, The Fluidyne Heat Engine--How to Build One, How it Works, National Technical Information Service, Springfield, VA, AD A006367 (1974).*

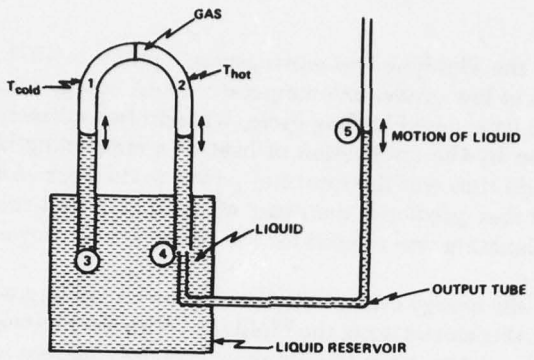

Figure 1. Schematic of Fluidyne pump.

The startup and subsequent sustained oscillations may be described physically in five steps (fig. 2).

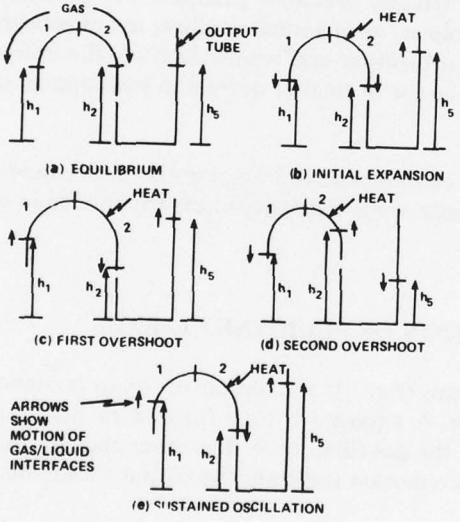

Figure 2. Schematic representation of Fluidyne startup process.

a. In equilibrium conditions, no heat is applied. The liquid levels h_1, h_2, and h_5 are prescribed by the static pressure in the gas volume of columns (1) and (2), and $h_1 = h_2$. (If the gas pressure p_{12} is ambient, p_∞, then all three levels are equal.)

b. Heat is applied to the right half of the gas volume of column (2). The gas expands, and the gas volume, V_G, increases while the gas pressure p_{12} also increases. As a natural consequence, liquid levels h_1 and h_2 decrease, and liquid level h_5 increases as the liquid in the displacer is accelerated. The gas temperature rises in column (2).

c. The inertia of the liquid in the output tube keeps the liquid moving; hence, the liquid in column (2) tends to keep moving downward, also. As more hot side is exposed, the liquid is accelerated further until equilibrium in the gas is reached.

d. Gravity stops the upward motion of liquid level h_1, and levels h_2 and h_5 tend to seek equality. Hence h_2 increases, and h_5 starts to decrease. At the same time, there is a reduction of hot volume. This reduction starts an overall gas volume decrease due to a temperature reduction since less gas is exposed to the heat source. The pressure p_{12} decreases. All this action is augmented by the descent of the output level due to gravity, which produces a dynamic head at the base of column (2), further increasing h_2. An overshoot of the two liquid levels occurs, $h_2 > h_1$, $h_2 > h_5$. This overshoot gives rise again to a gravity potential between liquid levels.

e. The liquid levels again seek equilibrium with level h_2 decreasing. This decrease exposes more of the gas to the heat source and causes the gas to expand; the cycle begins all over again, with the output liquid again moving upward.

This is the physical description as observed in a glass or plastic demonstration model built and tested during this program.

3. MATHEMATICAL MODEL

Geisow[4] has proposed a set of governing equations for a lossless Fluidyne system in an attempt to compute the conditions required for the onset of instability. To this end, he used the Euler equations of motion in one dimension, linearized them, and then performed a first-order perturbation stability analysis. The results of this analysis led to an expression for the critical temperature differential, ΔT, as a function of the pump geometry and for the oscillating frequency, ω. This is given as equations (1) and (1a):

$$\frac{\Delta T}{T_1 + T_2} = \frac{\rho g V_e}{2 A_D P_\infty} \left(\frac{\ell_c - \ell_h}{\ell_D} \right) , \qquad (1)$$

$$\omega = \left[2g \Big/ \left(2\ell_h + \ell_D A_c / A_D \right) \right]^{\frac{1}{2}} , \qquad (1a)$$

[4] *A. D. Geisow, The Onset of Oscillations in a Lossless Fluidyne, United Kingdom Atomic Energy Authority, Harwell, UK, AERE-M-2840 (October 1976).*

where

T_1 = cold temperature (K),

T_2 = hot temperature (K),

ρ = liquid density (kg/m^3),

g = acceleration of gravity (m/s^2),

V_e = equilibrium volume of gas (m^3),

A_D = cross-sectional area of displacer tube (m^2),

P_∞ = atmospheric pressure (Pa),

ℓ_c = equilibrium length of cold leg to output (m),

ℓ_h = equilibrium length of hot leg to output (m),

ℓ_D = length of displacer (m),

A_c = cross-sectional area of cold leg.

This analysis was performed for the geometry shown in figure 3 and indicates a strong dependency of system response on the displacer tube.

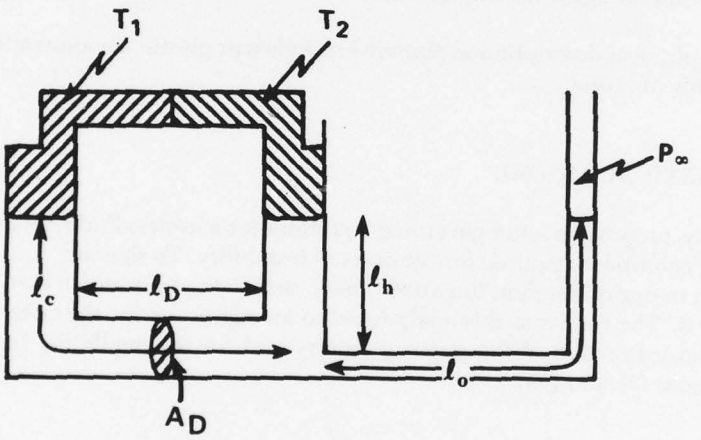

Figure 3. Schematic of Fluidyne II used by Geisow (AERE-M-2840, October 1976).

The original Fluidyne proposed by West[1] and described by Elrod[3] did indeed have such a configuration; however, currently commercially available Fluidynes[5] replace the displacer tube with a fluid reservoir as shown in figures 1 and 4.

---

[1] *C. West, The Fluidyne Heat Engine, United Kingdom Atomic Energy Authority, Harwell, UK, AERE-R-6775 (1971).*

[3] *H. Elrod, The Fluidyne Heat Engine--How to Build One, How it Works, National Technical Information Service, Springfield, VA, AD A006367 (1974).*

[5] *Stirling-Cycle Engines Developed at Harwell--The Fluidyne 3 Pump, United Kingdom Atomic Energy Authority, Harwell, UK, Harwell Design Studios 56/1975 (1975).*

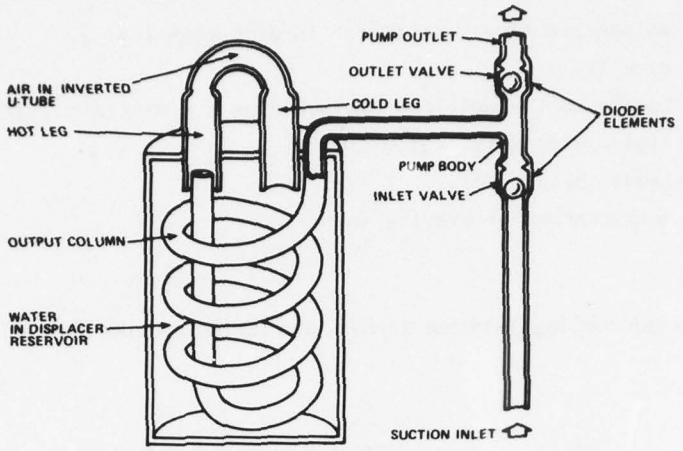

Figure 4. Schematic of actual Fluidyne pump (diode elements—ball valves—permit unidirectional flow).

Interestingly enough, the models shown by Elrod[3] always have the output tube axially in line with the hot leg as opposed to being at right angles as shown in figure 3, even when the displacer is present. This leads to the observation of section 2 that dynamic head feedback from the output to the hot leg is important in the pump operation in that the inertia of the moving fluid in the output leg preferentially acts to increase the head in the hot leg.

The following set of governing equations may be generated, assuming slug flow in all tubes for the geometry of figure 1 or 4.

The pressure drop, $\Delta P_{ij} = P_i - P_j$, for any tube is given by the electrical analog equation for time varying slug flow[6] (derived from the Euler equation):

$$\Delta P_{ij} = L_{ij} \frac{dQ_{ij}}{dt} + R_{ij} Q_{ij} + h_i \rho_L g \qquad (2)$$

where

L_{ij} = liquid inductance (kg/m^4) between points i and j, = $\rho_L \ell_{ij} / A_{ij}$,

ρ_L = liquid density (kg/m^3),

ℓ_{ij} = tube length between i and j (m),

A_{ij} = tube cross-sectional area (m^2),

[3] *H. Elrod, The Fluidyne Heat Engine--How to Build One, How it Works, National Technical Information Service, Springfield, VA, AD A006367 (1974).*

[6] *J. M. Kirshner, Fluid Amplifiers, McGraw-Hill Book Co, New York (1967).*

Q_{ij} = volumetric flow rate (m^3/s) in direction i to j,

t = time (s),

R_{ij} = liquid resistance (for laminar flow $R = 8\pi\mu\ell/A^2$) $[kg/(m^4 \cdot s)]$,

μ = liquid viscosity $[kg/(m \cdot s)]$,

h_{ij} = liquid height (m),

g = acceleration of gravity (m/s^2).

Therefore, for the cold leg, between steps (a) and (c) the pressure drop is

$$p_3 - p_1 = L_{13} \frac{dQ_{31}}{dt} + R_{31}Q_{31} + h_1\rho_L g \quad . \tag{3}$$

Similarly, the hot leg pressure drop can be written when the additional total pressure feedback term is included due to the dynamic head effect of the output leg:

$$p_4 - p_2 = L_{42} \frac{dQ_{42}}{dt} + R_{42}Q_{42} + h_2\rho_L g - \frac{\rho_L}{2} K_1 \left(\frac{Q_{45}}{A_{45}}\right)^2 \quad , \tag{4}$$

where

$$K_1 = 0,\ Q_{45} > 0;\ K_1 = 1,\ Q_{45} < 0.$$

Finally, the output leg presure drop is, with hot leg feedback,

$$p_4 - p_5 = L_{45} \frac{dQ_{45}}{dt} + R_{45}Q_{45} + h_5\rho_L g - \frac{\rho_L}{2} K_2 \left(\frac{Q_{42}}{A_{42}}\right)^2 \quad , \tag{5}$$

where

$$K_2 = 0,\ Q_{42} > 0;\ K_2 = 1,\ Q_{42} < 0.$$

The equation relating the liquid height and the volume flow rate is the constitutive equation

$$A \frac{dh}{dt} = Q \quad . \tag{6}$$

Hence, the individual time rates of height change are

$$\frac{dh_1}{dt} = \frac{Q_{31}}{A_{31}} \quad , \tag{7}$$

$$\frac{dh_2}{dt} = \frac{Q_{42}}{A_{42}} \quad , \tag{8}$$

$$\frac{dh_5}{dt} = \frac{Q_{45}}{A_{45}} \quad . \tag{9}$$

It follows, from conservation of mass of an incompressible liquid into the reservoir, that the net flow must be zero, or

$$- Q_{31} - Q_{42} - Q_{45} = 0 \quad . \tag{10}$$

Note the minus signs since each flow is assumed to be positive out of the reservoir. The pressure at the base of the cold leg is the reservoir pressure. If the output leg does not impede flow from the reservoir into it or the hot leg, then $p_3 = p_4$. If there is an orifice resistance, then

$$p_4 - p_3 = \frac{\rho_L Q_{31}^2}{2\left(A_{42} - A_{45}\right)^2 c_d^2} \quad , \tag{11}$$

where c_d is the discharge coefficient.

For convenience of this initial analysis, consider p_5 to be ambient:

$$p_5 = 101 \text{ kPa (absolute)} \quad . \tag{12}$$

We have up to this point 9 equations and 11 unknowns—namely, 5 pressures, 3 flows, and 3 heights; consequently, more equations are required.

If the assumption is made that the pressure is constant at any instant of time in the gas volume, which is a reasonable assumption considering that the process is relatively slow, the gaseous resistance of the tubing is negligible, and the head potential is likewise negligible, then another equation is available:

$$p_1 = p_2 \quad . \tag{13}$$

The gas mass must be conserved so that

$$m_1 + m_2 = \text{constant} \quad . \tag{14}$$

This equation has added two unknowns, m_1 and m_2, the masses of the cold and hot sides of the gas volumes (kg), respectively; hence, there are now 11 equations and 13 unknowns. The equation of state may be written for each side of the gas volume. If it is assumed that the gas is ideal, then

$$p_1 V_1 = m_1 R T_1 \quad , \tag{15}$$

$$p_1 V_2 = m_2 R T_2 \quad , \tag{16}$$

where

V_1 = volume of cold gas (m^3),
V_2 = volume of hot gas (m^3),
T_1 = temperature of cold gas (K),
T_2 = temperature of hot gas (K),
R = gas constant $[m^3/(s^2K)]$.

There are now 13 equations and 17 unknowns, the new unknowns being volumes V_1 and V_2 and temperatures T_1 and T_2.

The gas volumes are directly related geometrically to the position of the gas-liquid interface so that

$$V_1 = \frac{1}{2} V_e - (h_1 - h_e) A_{13} \quad . \tag{17}$$

and

$$V_2 = \frac{1}{2}V_e - (h_2 - h_e)A_{24} \quad , \tag{18}$$

where

$$h_e = \text{equilibrium height of liquid (m)} \quad .$$

This now brings us to 15 equations and 17 unknowns.

At this point, a statement can be made about temperatures T_1 and T_2. Elrod[3] and Geisow[4] chose to assume that the temperatures are known constants. This choice is tenuous since it requires that a step distribution in temperature exists in the gas tube. For the sake of simplicity, assume that

$$T_1 = \text{constant} \quad , \tag{19}$$

$$T_2 = \text{constant} \quad , \tag{20}$$

where T_1 and T_2 are average temperatures (K) in each volume of gas. These then bring the count of unknowns and equations even at 17 apiece. The evaluation of T_1 and T_2 is given in appendix A. Upon examination of the governing equations, one notes that the pressure drop equations are nonlinear since the inductance and the resistance terms are functions of the length of the liquid, which is variable. Linearization can be achieved by stipulating that the total excursions of the liquid interfaces be considerably smaller than the equilibrium lengths. For computer solution, however, this stipulation is not necessary. There are five independent first-order ordinary differential equations, since one of the flow equations is used to find a pressure. The solution of the entire set of equations gives the displacement of the output column of liquid. Since the object of this study is to establish the parameters relating to the efficiency of the pump, a quantity of interest is the output power, W. This is the time rate of increase of potential energy of the output or the root mean square (rms) value of the product of the flow and the dynamic head. The instantaneous power out is

$$W = \frac{1}{2}\left(\frac{Q_{45}}{A_{45}}\right)^2 Q_{45} \quad . \tag{21}$$

---

[3]*H. Elrod, The Fluidyne Heat Engine--How to Build One, How it Works, National Technical Information Service, Springfield, VA, AD A006367 (1974).*

[4]*A. D. Geisow, The Onset of Oscillations in a Lossless Fluidyne, United Kingdom Atomic Energy Authority, Harwell, UK, AERE-M-2840 (October 1976).*

The useful power is the rms value or

$$W_{rms} = 0.707 W_{max} \quad . \tag{22}$$

The input energy is the heat input from which the temperature distribution was obtained (app A).

Physical observations indicate that most of the losses occur in the input of heat to the system.

Equations (3) to (20) may now be cast into a computer program and solved simultaneously without resorting to perturbation or threshold analyses. This simultaneity is important because the actual values of displacements are needed to compute the output power.

4. NUMERICAL RESULTS

The computer program is given in appendix B with a sample printout. Figures 5 to 8 plot the various parameters of interest for typical geometries in which oscillations are self-sustained.

In figure 5, the three liquid displacements, the gas pressure, and the change of gas volume are shown as a function of time. They are in substantial agreement with the descriptive model

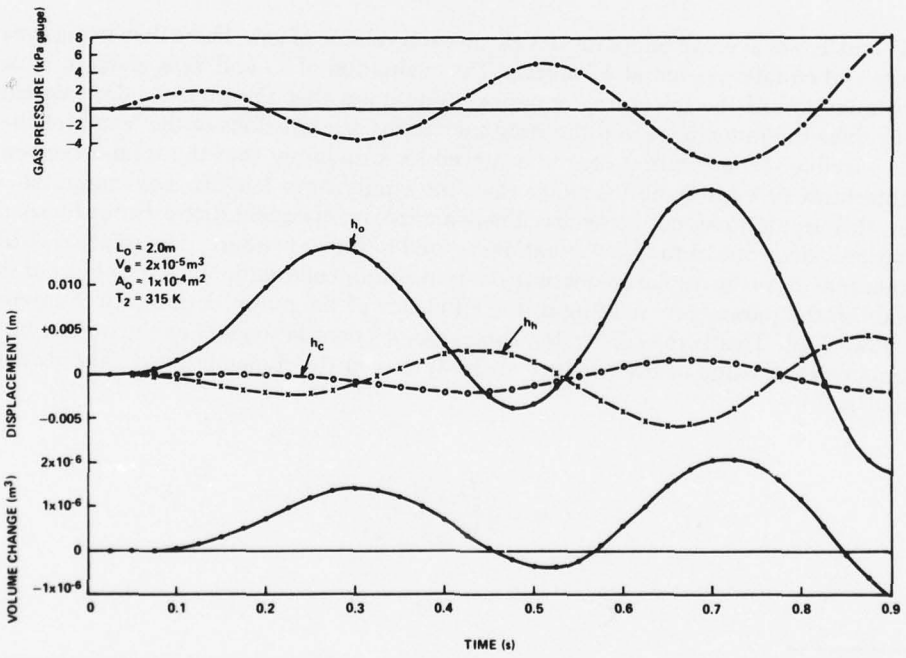

Figure 5. Time history of Fluidyne response: L_o = liquid inductance output, V_e = volume equilibrium, A_o = output area, T_2 = temperature of hot side of gas-liquid interface, and h = height of liquid.

proposed as a result of physical observations. Constant temperature apparently causes the oscillations to keep growing. For limit cycling, a more comprehensive, flow dependent temperature distribution has to be developed that in effect provides a time delay in the temperature change. The heat conduction time constant for air is $\tau = \varrho c_p r^2/k \approx 7$ s, where c_p = specific heat at constant pressure (W·s/kgK), r = radius of the pipe (m), and k = thermal conductivity (W/mK). Hence, it is a poor assumption that the temperature reaches the hot or cold value instantaneously, especially since the period of oscillations is an order of magnitude less than 7.0 s. Similarly, the convective time constant due to the movement of the gas-liquid interface must be of the same order, that is, 1 s. Due to the complexity of the fluid mechanic-heat transfer governing equations for such a phenomenon, this development must be left to a more comprehensive and detailed analysis at a later time.

In figure 6, one sees the variation of amplitude and frequency of oscillation for different parametric changes. If one observes the lower three sets of curves, the effect of increasing the output length can be seen. As one would expect, the period increases with output length due to increased inductance.

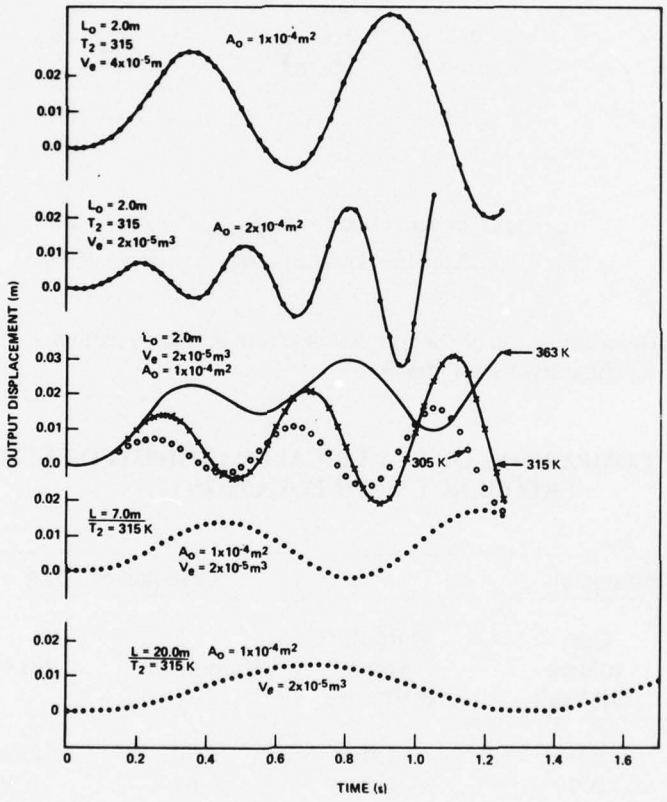

Figure 6. Output displacements for various parameters: L_o = liquid inertance output, T_2 = temperature of hot side of gas-liquid interface, V_e = volume equilibrium, and A_o = output area.

The middle set of curves demonstrates the effect of increasing the hot side temperature. The frequency decreases slightly with increasing temperature. This decrease is a result of the higher mean pressure in the gas volume that results in a larger volume and, hence, a slightly increased gas capacitance. Interestingly, the amplitude appears to have a maximum at a midrange temperature.

The curve marked "305" shows the effect of increasing the output area. This increase has the effect of decreasing the inductance, again increasing the frequency.

The top curve of figure 6 shows the effect of increasing the inital gas volume and the mass. The gas volume, as already suspected, acts as a capacitance; hence, increasing the capacitance decreases the frequency, as demonstrated in the figure.

Intuitively, one would expect that the predominant frequency determining terms are the output inductance and the gas capacitance. This would lead to the assumption that the system frequency, f, should behave approximately as an RLC circuit, so that

$$f = \frac{1}{2\pi\left(L_o C_G\right)^{\frac{1}{2}}} \quad , \tag{23}$$

where

C_G = gas capacitance = V_e/p_∞ $(m^4 s^2/kg)$,

p_∞ = equilibrium absolute gas pressure (Pa) .

Table I shows the comparison of the frequencies from equation (23) with the actual numerical results obtained from the curves in figure 6.

TABLE I. COMPARISON OF NUMERICALLY COMPUTED FLUIDYNE FREQUENCY WITH EQUATION (23)

Parameter			Frequency (Hz)		
Output length (m)	Gas volume ($\times 10^{-5}$ m^3)	Output area ($\times 10^{-4}$ m^2)	Numerical	Eq (23)	Case No.
2.0	2.0	1.0	2.50	2.5299	1
7.0	2.0	1.0	1.54	1.3520	2
20.0	2.0	1.0	0.77	0.7997	3
2.0	4.0	1.0	1.74	1.7883	4
2.0	2.0	2.0	3.33	3.5766	5

Note: Liquid density ϱ_L = 1000 kg/m³; ambient absolute pressure p_∞ = 101 kPa.

The agreement is good, so equation (23) may be used as a design guide for determining the operating frequency of a Fluidyne.

The question of cycle efficiency can be answered only by determining the nature of the thermodynamic cycle, the energy input, and the energy output. In figure 7, the relation between gas pressure and volume is shown for startup and the first cycle for case 1 of table I. It is immediately apparent that this is not a Stirling cycle as originally thought by the inventor.[1] Instead, it

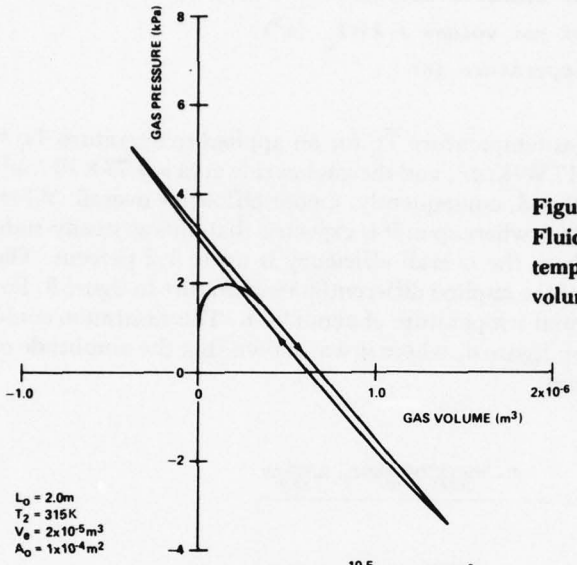

Figure 7. Pressure-volume diagram for first cycle of Fluidyne: L_o = liquid inertance output, T_2 = temperature of hot side of gas-liquid interface, V_e = volume equilibrium, and A_o = output area.

$$\text{AREA} = pV \quad \frac{10.5}{2} \times 0.1 \sim 0.525 \text{m}^2$$

$$\frac{2\ \text{kPa} \times 0.5 \times 10^{-6}\ \text{m}^3}{\text{m}^2} = 10^{-6}\ \frac{\text{kPa m}^3}{\text{m}^2} \times 10^3\ \frac{\text{Pa}}{\text{kPa}}$$

$$= 10^{-3}\ \frac{\text{Pa m}^3}{\text{m}^2}$$

$$pV = 0.525 \times 10^{-3}\ \text{Pa m}^3$$

$$\tau = 1/f = 0.4\text{s}$$

$$\frac{\text{WORK}}{\text{TIME}} = 1.3125 \times 10^{-3}\text{W}$$

$$\text{RMS OUTPUT POWER FIRST CYCLE} = \left(\frac{0.332 + 0.122}{2}\right) \times 10^{-3}\text{W} \times 0.707$$

$$= 0.16225 \times 10^{-3}\text{W}$$

$$\therefore\ \eta = 12.36\%$$

resembles more a Carnot cycle, albeit it is not that, either. The observed efficiency of the Fluidyne's first cycle is 12.36 percent when defined as the output power divided by the power of one cycle ($\int p\, dV$). The heat input to the gas gives the overall efficiency. The heat input may be approximated by the convective heat transfer equation and the mean gas temperature $\overline{T}_h$ as computed in appendix A:

[1] *C. West, The Fluidyne Heat Engine, United Kingdom Atomic Energy Authority, Harwell, UK, AERE-R-6775 (1971).*

$$Q_{in} = HA\left(T_h - \bar{T}_h\right) \quad , \tag{24}$$

where

H = convective heat transfer coefficient ($W/K/m^2$),

A = outside area of hot volume = $2\pi r \ell_G$ (m^2),

T_h = applied hot temperature (K) .

For the case in question, the average gas temperature $\overline{T}_h$ for an applied temperature T_h = 315 K is 313.454 K. An average value of H = 17 W/K/m², and the gas hot side area is 3.77×10^{-3} m². These values result in a heat input of 0.21 W and, consequently, a poor efficiency overall. When the pump is allowed to operate for three cycles, whereupon it is expected that almost steady-state conditions would normally have been reached, the overall efficiency is up to 1.2 percent. The third-cycle efficiency is shown as a function of the applied differential temperature in figure 8. For L_o = 2.0 m, there is a maximum at a differential temperature of about 24 K. This maximum could have been predicted by the observations from figure 6, where it was shown that the amplitude of oscillation was lower at elevated temperatures.

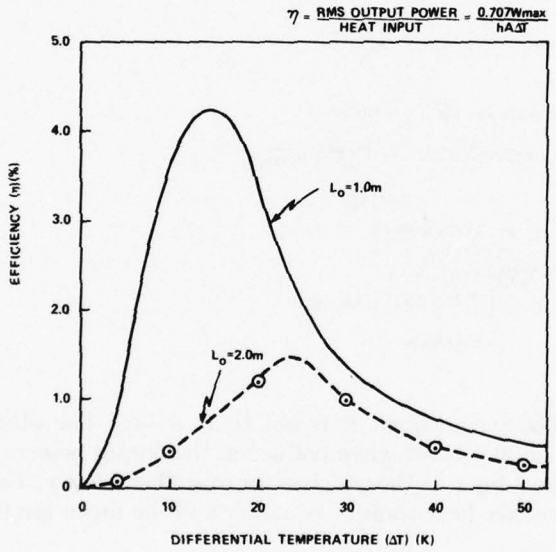

Figure 8. Fluidyne efficiency as function of input temperature and output length: h = height of liquid column and L_o = liquid inertance output.

Also, it can be observed in figure 6 that the amplitude of oscillation was inversely proportional to the output length; therefore, it seems intuitive that the efficiency increases if the output length decreases. When the gas volume increases, the amplitude also increases, but the frequency decreases. The efficiency may increase; however, since the frequency is lower, the output flow is lower, so the net effect is that the efficiency is not materially affected. Computed results (not shown here) bear out this thesis. Figure 8 shows, however, that efficiency is markedly improved by decreasing the output length. Also shown is that the optimum differential temperature is lowered by a factor of two as the maximum efficiency is more than doubled.

5. DISCUSSION AND CONCLUSIONS

The disturbing point in this analysis is the exponential growth of oscillations. Appendix A discusses this growth and the temperature distribution. More fundamentally, however, the reason for this growth is probably the assumption that the gas changes temperature instantaneously from hot to cold or vice versa. It takes an infinite amount of power or energy to raise a finite amount of mass a finite temperature in zero time. In a numerical model, this infinity is tempered, but still remains large. The conclusion to be drawn, therefore, is that the gas must be much more carefully modeled.

The values of efficiency presented here cannot be used in anything more than a comparative sense since they are based on output power values that are steadily increasing. Observations, however, have indicated that the actual process reaches a steady state after about three cycles. Since the frequencies computed are close to those observed and the amplitudes are reasonable, the three-cycle numerical results have been used.

Two efficiencies are involved, thermodynamic and mechanical. Thermodynamic efficiency is relatively low, and mechanical efficiency, although an order of magnitude greater than thermodynamic, is still only about 10 percent. Thus, the low efficiencies reported are substantiated by this numerical analysis. There is hope, however, of improving the overall efficiency by a factor of two or even three over the extant devices by a thorough parametric study. This study has examined more than 2500 permutations of geometry, and they cannot be presented here. The important observations, however, have been presented, and hope for better efficiency is offered.

Several conclusions may be drawn from this study. The Fluidyne pump operates not, as first thought, on a Stirling cycle, but on a cycle more closely resembling a Carnot cycle. It is essentially a low-efficiency device, although overall thermal efficiencies of 10 percent may conceivably be reached. Poor thermal coupling with the gas accounts for a large portion of this inefficiency. In the real device, it would be advantageous to have a nonconducting liquid and a highly conducting gas (a contradiction of thermodynamic terms). This advantage could possibly be realized by providing an insulating interface substance such as foam. The gas volume should be insulated so that all the heat input stays in the gas.

Relating to the analysis itself, the important points and parameters have been identified. The displacer of the original Fluidyne has been shown to be superfluous to the device. Although amplitude oscillations were never constant, limit cycling might occur when the temperature distribution is corrected or modeled more appropriately. A simple model for the frequency of the

Fluidyne has been proposed that relates the gas volume to the geometry of the output tube in terms of an electrical RLC second-order system analogy. Good agreement with numerical results has been demonstrated.

The overall objectives of this study were to determine if the efficiency of existing Fluidynes could be increased and to comprehensively describe the physics of the Fluidyne operation. These objectives have been met. The efficiency may be increased by appropriate geometric choices, and for the first time a clear description has been proposed for the operation.

Research and development of the Fluidyne heat engine should continue. The Fluidyne can provide fluid power with tiny temperature differentials, with no moving parts. For power production in inaccessible locations, this device is ideal. One of the most inaccessible places is the interior core of the pressure vessel of a nuclear reactor. The nuclear community requires redundant and completely independent safety, monitoring, and control systems. Presently, all backup controls depend on a single type of energy source—electricity. Should this ever fail, then no systems other than the purely mechanical ones could operate. The mechanical systems normally can provide only shutdown capability. A fluidic system, self-contained within the reactor core, with no pressure vessel penetrations, powered by the rectified output of a Fluidyne can provide all the active monitoring and control of the standard systems and also cause shutdown in the event of a scram. This approach can avoid the costly and inconvenient automatic shutdowns presently envisioned. A reactor may continue to operate with the fluidic system installed.

Recent panel discussions sponsored by the American Society of Mechanical Engineers (ASME)* on fluidics and nuclear engineering specifically mentioned fluidic shutdown schemes being developed in the United States. At the same session, fluidic two-diode pumping systems were described that have been developed for the United Kingdom Atomic Energy Authority. These fluidic diode systems have successfully operated with Fluidyne pumps at Harwell. C. F. King of the University College, Cardiff, UK, reported that newly developed vortex diodes that have turndown ratios in excess of 30:1 operate exceptionally well when attached to the Fluidynes. For a session on energetics, fluidic temperature sensors that can withstand extremely hot, harsh environments were reported by Drzewiecki et al.[7] Such sensors are ideal candidates for use with a Fluidyne system for the monitoring of nuclear, fossil fuel, solar, and geothermal power generation plants. Of particular interest are military nuclear power facilities. These are normally mobile and do not have a ready source of auxiliary power to operate secondary systems. Even when they do, the proximity of such auxiliary systems makes them vulnerable to failure due to either the military environment or the radiation possibility from the primary plant itself. The Fluidyne offers a unique solution to this problem. It merely becomes an integral part of the whole.

---

*T. M. Drzewiecki, *Fluidic Applications in Nuclear Engineering*, ASME Winter Annual Meeting, Atlanta, GA (November 1977).

[7]T. M. Drzewiecki, R. M. Phillippi, and C. Paras, *Fluidics--A New Potential for Energy Conservation by Continuous High Temperature Monitoring and Control*, Heat Transfer in Energy Conservation, R. J. Goldstein et al, ed., ASME Book H00106, New York (November 1977), 127-134.

Other military applications for remotely powered fluidic systems are battlefield security and sensor systems (REMBASS). Fluidic sensors have been demonstrated to be uniquely suited to the battlefield. The source of power has been of concern, however. A Fluidyne that can operate on a 3- or 4-deg temperature difference could operate during the day on light energy and during the night on the stored heat in the ground with the colder night air being the thermal sink. This discussion is limited only by imagination. It is the author's opinion that many military systems problems can be effectively and efficiently solved by fluidic, flueric, or fluid systems powered by Fluidyne pumps.

LITERATURE CITED

(1) C. West, The Fluidyne Heat Engine, United Kingdom Atomic Energy Authority, Harwell, UK, AERE-R-6775 (1971).

(2) C. West, And Yet It Moves, New Scientist, 29 (August 1974).

(3) H. Elrod, The Fluidyne Heat Engine--How to Build One, How it Works, National Technical Information Service, Springfield, VA, AD A006367 (1974).

(4) A. D. Geisow, The Onset of Oscillations in a Lossless Fluidyne, United Kingdom Atomic Energy Authority, Harwell, UK, AERE-M-2840 (October 1976).

(5) Stirling-Cycle Engines Developed at Harwell--The Fluidyne 3 Pump, United Kingdom Atomic Energy Authority, Harwell, UK, Harwell Design Studios 56/1975 (1975).

(6) J. M. Kirshner, Fluid Amplifiers, McGraw-Hill Book Co, New York (1967).

(7) T. M. Drzewiecki, R. M. Phillippi, and C. Paras, Fluidics--A New Potential for Energy Conservation by Continuous High Temperature Monitoring and Control, Heat Transfer in Energy Conservation, R. J. Goldstein et al, ed., ASME Book H00106, New York (November 1977), 127-134.

NOMENCLATURE

A	area (m^2)
c_d	discharge coefficient (-)
c_p	specific heat at constant pressure (W·s/kgK)
C	capacitance (m^4s^2/kg)
f	frequency (Hz)
g	acceleration of gravity (m/s^2)
h	height of liquid column (m)
H	convective heat transfer coefficient ($W/K/m^2$)
k	thermal conductivity (W/mK)
K	constant, =1 when $Q < 0$; =0 when $Q > 0$
ℓ	column length (m)
L	liquid inertance (inductance) (kg/m^4)
m	mass (kg)
p	absolute pressure (Pa)
P	pressure (Pa)
Q	volumetric flow rate (m^3/s)
r	radius of pipe (m)
R	liquid resistance $[kg/(m^4 \cdot s)]$
R	gas constant $[m^3/(s^2K)]$
t	time (s)
T	absolute temperature (K)
$\bar{T}$	mean gas temperature
u	liquid velocity (m/s)
V	volume (m^3)
W	power (W)
Δ	change
μ	fluid absolute viscosity $[kg/(m \cdot s)]$
η	efficiency
ρ	liquid density (kg/m^3)
τ	time constant (s)
ω	radian oscillating frequency (rad/s)

Subscripts

c	cold
D	displacer
e	equilibrium
G	gas
h	hot
i	integer
in	input
j	integer
L	liquid
max	maximum
o	output
rms	root mean square average
1	cold side of gas-liquid interface
2	hot side of gas-liquid interface
3	cold side of tube lower end
4	hot side of tube lower end, entrance to output tube node
5	output tube exit
∞	ambient, atmospheric

APPENDIX A.--TEMPERATURE DISTRIBUTION IN AN ENCLOSED CYLINDRICAL GAS VOLUME

APPENDIX A

The gas volume that provides the means for the motive power in the Fluidyne is essentailly cylindrical. It is bounded on either end by liquid interfaces that move so that the volume of gas expands and contracts. Heat is applied to one half and rejected from the other half by maintaining essentially constant hot and cold wall temperatures, T_h and T_c, respectively. Consider, therefore, two touching cylinders with constant wall and end temperatures. The end temperatures can be justified to be T_h or T_c if the conductivity of the liquid is much greater than that of the gas. Figure A-1 shows the assumed geometry.

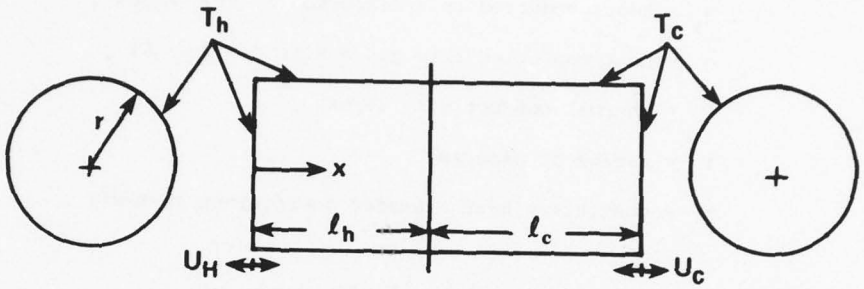

Figure A-1. Schematic of gas volume.

Assume one-dimensional heat flow in the x-direction, and further assume that heat enters the volume by natural convection from the wall temperatures. In the first instance, neglect any motion of the interfaces, and compute the static temperature distribution. For an infinitesimal slice of the volume of length dx, the heat balance is shown in figure A-2.

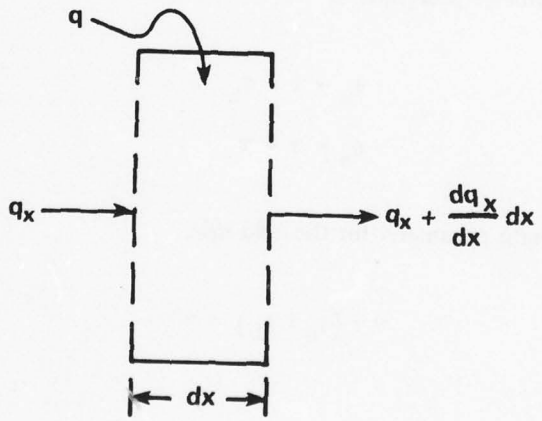

Figure A-2. Heat balance in differential element.

APPENDIX A

The heat balance is

$$q_x - \left(q_x + \frac{dq_x}{dx}\,dx\right) + q = 0 \quad , \tag{A-1}$$

where

q_x = heat conducted in x-direction = $-k\pi r^2\, dT/dx$,

q = heat convected into gas = $H2\pi r\, dx\, (T_h - T)$,

k = thermal conductivity (W/mK) ,

r = radius of pipe (m) ,

H = convective heat transfer coefficient ($W/K/m^2$) .

The governing differential equations for the hot and cold columns are

$$\frac{d^2T}{dx^2} + \frac{2H}{kr}\,(T_h - T) = 0 \quad , \tag{A-2}$$

$$\frac{d^2T}{dx^2} + \frac{2H}{kr}\,(T_c - T) = 0 \quad . \tag{A-3}$$

A new temperature parameter is defined as

$$\theta_h = T - T_h \quad , \tag{A-4}$$

$$\theta_c = T - T_c \quad . \tag{A-5}$$

In addition, define a length parameter for the cold side,

$$y = \left(\ell_c + \ell_h\right) - x \quad , \tag{A-6}$$

and let

$$\lambda^2 = 2H/kr \quad . \tag{A-7}$$

The governing equations thus become

$$\frac{d^2\theta_h}{dx^2} - \lambda^2\theta_h = 0 \quad , \tag{A-8}$$

$$\frac{d^2\theta_c}{dy^2} - \lambda^2\theta_c = 0 \quad . \tag{A-9}$$

The solutions of equations (A-4) to (A-9) are

$$\theta_h(x) = B_1 \sinh \lambda x + B_2 \cosh \lambda x \quad , \tag{A-10}$$

$$\theta_c(y) = B_3 \sinh \lambda y + B_4 \cosh \lambda y \quad . \tag{A-11}$$

The boundary conditions are

$$T(x=0) = T_h \quad ,$$

$$T\left(x=\ell_c+\ell_h\right) = T_c \quad ,$$

$$T_h\left(x=\ell_h\right) = T_c\left(x=\ell_h\right) \quad ,$$

$$\frac{dT_h\left(x=\ell_h\right)}{dx} = \frac{dT_c\left(x=\ell_h\right)}{dx} \quad .$$

In terms of the new parameters,

$$\theta_h(0) = 0 \quad , \tag{A-12}$$

$$\theta_h\left(\ell_h\right) = \theta_c\left(\ell_c\right) + T_c - T_h \quad , \tag{A-13}$$

$$\frac{d\theta_h}{dx}\left(\ell_h\right) = -\frac{d\theta_c}{dy}\left(\ell_c\right) \quad , \tag{A-14}$$

$$\theta_c(0) = 0 \quad . \tag{A-15}$$

APPENDIX A

Equations (A-12) and (A-15) make $B_2 = B_4 = 0$. If now ℓ_c is assumed equal to ℓ_h (on the average), then by symmetry equations (A-13) and (A-14) may be replaced if

$$T\left(x=\ell_h\right) = \frac{T_h + T_c}{2} \quad .$$

Thus,

$$\theta_h\left(\ell_h\right) = \frac{T_c - T_h}{2}$$

and

$$\theta_c\left(\ell_c\right) = \frac{T_h - T_c}{2} \quad ,$$

so that

$$\theta_h(x) = \frac{\left(T_c - T_h\right) \sinh \lambda x}{2 \sinh \lambda \ell_h} \quad , \tag{A-16}$$

$$\theta_c(y) = \frac{\left(T_h - T_c\right) \sinh \lambda y}{2 \sinh \lambda \ell_c} \quad . \tag{A-17}$$

For the analysis, average values may be used so that

$$\bar{T}_h = T_h + \frac{1}{\ell_h} \int_o^{\ell_h} \theta_h(x)\, dx$$

and

$$\bar{T}_c = T_c + \frac{1}{\ell_c} \int_o^{\ell_c} \theta_c(y)\, dy \quad .$$

When equations (A-16) and (A-17) are substituted and the indicated integrations are performed, the results are

$$\bar{T}_h = T_h + \frac{T_c - T_h}{2\lambda \ell_h \sinh \lambda \ell_h} \left(\cosh \lambda \ell_h - 1\right) \tag{A-18}$$

and

$$\bar{T}_c = T_c + \frac{T_h - T_c}{2\lambda \ell_c \sinh \lambda \ell_c} \left(\cosh \lambda \ell_c - 1\right) \quad . \tag{A-19}$$

These average temperatures are used in the numerical model.

A more sophisticated model assumes that the hot side liquid is asymptotically cold. In this model, there are three temperature zones. The formulation is the same for equations (A-18) and (A-19), except that the simplifying assumption of symmetry is not used. The solutions only are given here:

$$T_L(x) = B_1 e^{\lambda_L x} + T_c \quad ,$$

$$T_h(x) = B_1 \frac{\lambda_L}{\lambda_G} \sinh \lambda_G x + \left(B_1 + T_c - T_h\right) \cosh \lambda_G x + T_h \quad ,$$

$$T_c(x) = B_5 \sinh \left[\lambda_G \left(\ell_c + \ell_h - x\right)\right] + T_c \quad ,$$

$$B_1 = \frac{1}{B}\left(T_h - T_c\right)\left[\cosh \lambda_G \ell_h - 1 + \tanh \left(\lambda_G \ell_c\right) \sinh \lambda_G \ell_h\right] \quad ,$$

$$B = \frac{\lambda_L}{\lambda_G} \sinh \lambda_G \ell_h + \cosh \lambda_G \ell_h + \frac{1}{\lambda_G} \tanh \lambda_G \ell_c \left(\lambda_L \cosh \lambda_G \ell_h + \lambda_G \sinh \lambda_G \ell_h\right) ,$$

$$B_5 = \frac{B_1\left(\frac{\lambda_L}{\lambda_G} \sinh \lambda_G \ell_h + \cosh \lambda_G \ell_h\right) + \left(T_c - T_h\right)\left(\cosh \lambda_G \ell_h - 1\right)}{\sinh \lambda_G \ell_c} \quad ,$$

and the average hot and cold temperatures are

$$\bar{T}_h = T_h + \frac{B_1 \lambda_L}{\lambda_G^2 \ell_h} \left(\cosh \lambda_G \ell_h - 1\right) + \frac{B_1 + T_c - T_h}{\lambda_G \ell_h} \sinh \lambda_G \ell_h \quad ,$$

$$\bar{T}_c = T_c + \frac{B_5}{\lambda_G \ell_c} \left(\cosh \lambda_G \ell_c - 1\right) \quad ,$$

APPENDIX A

where

T_L = temperature of liquid ,

G = gas ,

ℓ_c = length of cold column ,

ℓ_h = length of hot column ,

B_i = constant of integration .

Even more sophistication may be introduced by dropping the one-dimensional restriction. Dropping it leads to two governing equations,

$$\frac{\partial^2 \theta_i}{\partial \xi^2} + \left(\frac{\ell_h + \ell_c}{R}\right)^2 \frac{\partial^2 \theta_i}{\partial \Psi^2} + \left(\frac{\ell_h + \ell_c}{R}\right)^2 \frac{1}{\Psi} \frac{\partial \theta_i}{\partial \Psi} = 0 ,$$

where

$$\theta_i = \frac{T - T_c}{T_h - T_c} ,$$

$$\xi = x \Big/ \left(\ell_h + \ell_c\right) ,$$

R = liquid resistance,

$\Psi = r/R$,

$i = L, G$,

with these boundary conditions on the liquid:

$$\theta_L(\xi, 1) = 0 ,$$

$$\theta_L(-\infty, \Psi) = 0 ,$$

$$\frac{\partial \theta_L}{\partial \Psi}(\xi, 0) = 0 ,$$

$$\theta_L(0, \Psi) = \theta_G(0, \Psi) ;$$

and with these boundary conditions on the gas:

$$\theta_G(\xi,1) = \begin{cases} 1, & 0 \le \xi < \ell_h \Big/ \left(\ell_h + \ell_c\right) \\ 0, & \xi \ge \ell_h \Big/ \left(\ell_h + \ell_c\right) \end{cases} ,$$

$$\frac{\partial \theta_G}{\partial \Psi} (\xi,0) = 0 \quad ,$$

$$\frac{\partial \theta_G}{\partial \xi} (0,\Psi) = \frac{\partial \theta_L}{\partial \xi} (0,\Psi) \quad ,$$

$$\theta_G(1,\Psi) = 0 \quad .$$

These equations may be solved by separation of variables and lead to two eigenvalue problems resulting in a double infinite series in hyperbolic functions and Bessel functions. This tedious solution is left for the reader if he should desire to pursue it.

The original differential equations (A-2) and (A-3) are altered when gaseous motion is considered. Equation (A-3) becomes

$$\frac{d^2T}{dx^2} + \frac{2H}{Rk} \left(T_h - T\right) - \frac{\Psi c_p u}{k} \frac{dT}{dx} = 0 \quad , \qquad \text{(A-20)}$$

where u = liquid viscosity. If one assumes that the initial static temperature distribution is developed prior to any volume change (gas velocity onset), equation (A-20) may be used to examine the relative importance of the convective and conductive terms. Assume that a temperature distribution exists. Assign order of magnitude values to the derivatives:

$$\frac{dT}{dx} \sim \frac{T_h - T_c}{\ell_h} \quad ,$$

$$\frac{d^2T}{dx^2} \sim \frac{T_h - T_c}{\ell_h^2} \quad .$$

For the conductive term d^2T/dx^2 to be negligible compared with the convective term $(\Psi c_p u/k)\, dT/dx$,

$$\frac{d^2T}{dx^2} << \frac{\Psi c_p u}{k} \frac{dT}{dx} \quad ,$$

or

$$\frac{\Psi c_p u \ell_h}{k} >> 1 \quad . \tag{A-21}$$

For air,

$\Psi = 1.2$ kg/m^3 ,

$c_p = 1.05 \times 10^3$ W·s/kgK, specific heat at constant pressure,

$\ell_h = 0.1$ m ,

$k = 0.026$ W/mK, thermal conductivity .

For the velocity, assume sinusoidal displacement of ±0.02 m at 3 Hz, so that the maximum velocity is $2\pi f(0.02) = 0.38$ m/s. Therefore,

$$\frac{\Psi c_p u \ell_h}{k} = 1841 >> 1 \quad .$$

This indicates that during oscillation there is no significant effect of conduction; consequently, if the gas volume moves back and forth as a slug, the temperature is governed only by

$$\frac{d\theta}{dx} + \frac{\Psi c_p u R}{2H} \theta = 0 \quad ,$$

which implies that

$$\theta = B_6 \exp\left(- \frac{\Psi c_p u R}{2H} x\right) \quad ,$$

and if the boundary condition is that $\theta = 0$, then $B_6 = 0$, and the temperature remains at its initial constant value.

In reality, the volume expands and contracts, and there is conduction with a lag time, so that the initial temperature distribution eventually decays to a more uniform overall temperature due to the mixing effect of the convective terms. In addition, more complex boundary conditions exist. A thermal lag through the wall or the device supplies heat, and there is conduction axially in the walls. A considerable effort would have to be expended to thoroughly analyze the complete problem, given the velocity distribution. If we add now the complexity of coupling the transient

three-dimensional energy equation and the Navier-Stokes equations for the gas to the time-dependent oscillating liquid equations, the problem becomes massive.

A tentative time to solve such a problem is 1 to 2 man years. Such a solution would be highly desirable if any great effort or expenditure were ever contemplated for the Fluidyne.

APPENDIX B.--COMPUTER PROGRAM AND NUMERICAL RESULTS

APPENDIX B

This appendix presents the Fluidyne pump computer program written in FORTRAN IV for a 360/70 IBM computer. Five first-order differential equations are integrated by DVERK, an IBM supplied Runge-Kutta scheme that uses a fifth- and a sixth-order algorithm to reduce the global error to that specified by the user. It chooses the time increments within the desired steps of printout, which are specified by XEND. The program has five nested parameter DO loops that compute the response of the Fluidyne while the following parameters are swept:

Output length
Equilibrium liquid height
Equilibrium gas volume
Output area
Maximum hot temperature

All units are specified in SI units, except for the gas constant, which is in English customary units, but is converted in the program. All outputs are in SI units.

A sample printout is given for case 1 of table I in the main body of the report.

APPENDIX B

```
 01/04/78  13.12.17

FILE: FLUDYN   FORTRAN  P1                        NAVAL POSTGRADUATE SCHOOL

C THE PROGRAM FLUDYN SOLVES THE GOVERNING EQUATIONS FOR THE FLUIDYNE 3   FLU00010
C PUMP AS FORMULATED BY T. DRZEWIECKI ON 27 SEP 1977                     FLU00020
      DIMENSION Y(5),C(24),W(5,9)                                        FLU00030
      DIMENSION YPRIME(5)                                                FLU00040
      COMMON P4,P5,R45,RHOLIQ,G,A24,H45,P3,P1,R31,H13,A13,A45            FLU00050
      EXTERNAL FCN                                                       FLU00060
C   INPUT PARAMETERS: COLD TEMPERATURE,K;TEMPERATURE INCREMENT,K;        FLU00070
C   EQUILIBRIUM HEIGHTS,M;EQUILIBRIUM GAS VOLUME,M3;AMBIENT PRESSURE,KPA;FLU00080
C   COLD LEG AREA,M2;HOT LEG AREA,M2;OUTPUT LEG AREA,M2;COLD LEG LENGTH,MFLU00090
C   HOT LEG LENGTH,M;OUTPUT LEG LENGTH,M;LIQUID DENSITY,KG/M3;           FLU00100
C   GAS CONSTANT,FT-LBF/LBM-F;PI;LIQUID VISCOSITY,KG/M/S;MAXIMUM HOT LEG FLU00110
C   TEMPERATURE,K;GRAVITATIONAL CONSTANT,M2/S;TIME INCREMENT,S.          FLU00120
      READ(5,50) T1,DELT,HE,VE,P5,A13,A24,A45,HC,HH,HO,RHOLIQ            FLU00130
      READ(5,51) R,PI,VIS,TMAX,G,DT                                      FLU00140
      READ(5,52) K1                                                      FLU00150
      P5=P5*1000.                                                        FLU00160
      R=R*2.205*1.8*6.89*12000.*(.0254**3)                               FLU00170
      DO 60 JHO=1,10                                                     FLU00180
      HO=FLOAT(JHO)                                                      FLU00190
      WRITE(6,200) HO                                                    FLU00200
200   FORMAT('    HO=',F7.1)                                             FLU00210
      DO 61 JHE=1,4                                                      FLU00220
      HE=.1*FLOAT(JHE)                                                   FLU00230
      WRITE(6,201) HE                                                    FLU00240
201   FORMAT('    HE=',F7.2)                                             FLU00250
      DO 62 JVE=1,4                                                      FLU00260
      VE=.0001*FLOAT(JVE)                                                FLU00270
      WRITE(6,202) VE                                                    FLU00280
202   FORMAT('    VE=',F9.5)                                             FLU00290
      DO 63 JA45=1,3                                                     FLU00300
      A45=.0001*FLOAT(JA45)                                              FLU00310
      WRITE(6,203) A45                                                   FLU00320
203   FORMAT('  A45=',F9.5)                                              FLU00330
      DO 64 JTMAX=1,6                                                    FLU00340
      TMAX=295.+10.*FLOAT(JTMAX)                                         FLU00350
      WRITE(6,204) TMAX                                                  FLU00360
204   FORMAT(' TMAX=',F7.1)                                              FLU00370
      N=5                                                                FLU00380
      N=5                                                                FLU00390
C   INITIAL CONDITIONS                                                   FLU00400
      X=0.0                                                              FLU00410
      Y(1)=0.0                                                           FLU00420
      Y(2)=0.0                                                           FLU00430
      Y(3)=HE                                                            FLU00440
      Y(4)=HE                                                            FLU00450
      Y(5)=HE                                                            FLU00460
      T2=T1                                                              FLU00470
      D=158.*VE/A24                                                      FLU00480
      F=(SINH(D)-1.)/2./D/SINH(D)                                        FLU00490
      Y(1)=0.0                                                           FLU00500
      Y(2)=0.0                                                           FLU00510
      TOL=0.0001                                                         FLU00520
      IND=1                                                              FLU00530
      CVOL=F3*VE/R/T1                                                    FLU00540
C   COMPUTATION OF RESISTANCES AND INDUCTANCES                           FLU00550
C   AND GAS MASS.                                                        FLU00560
      WRITE(5,35)                                                        FLU00570
      WRITE(6,36)                                                        FLU00580
      DO 10 K=1,K1                                                       FLU00590
      R31=8.*PI*VIS*Y(3)/A13**2                                          FLU00600
      R24=8.*PI*VIS*Y(4)/A24**2                                          FLU00610
      R45=8.*PI*VIS*(HO-HE+Y(5))/A45**2                                  FLU00620
      H13=RHOLIQ*Y(3)/A13                                                FLU00630
      H24=RHOLIQ*Y(4)/A24                                                FLU00640
      H45=RHOLIQ*(HO-HE+Y(5))/A45                                        FLU00650
C   START COMPUTATION OF TIME VARYING SEQUENCE AND INTEGRATION OF THE DE-FLU00660
      XEND=FLOAT(K)*DT                                                   FLU00670
      V1=VE/2.-(Y(3)-HE)*A13                                             FLU00680
      V2=VE/2.-(Y(4)-HE)*A24                                             FLU00690
      V=V1+V2                                                            FLU00700
```

```
FILE: FLUDYN   FORTRAN  P1                    NAVAL POSTGRADUATE SCHOOL

      TC=T1+(T2-T1)*F                                                          FLUC0710
      TH=T2+(T1-T2)*F                                                          FLUC0720
      P1=GMASS*R*TC*TH/(V1*TH+V2*TC)                                           FLUC0730
      P2=P1                                                                    FLUC0740
      IF(Y(1).GT.0.0) GO TC 6                                                  FLUC0750
      B1=1.0                                                                   FLUC0760
      GO TO 7                                                                  FLUC0770
6     B1=0.0                                                                   FLUC0780
7     CONTINUE                                                                 FLUC0790
      P4=H24*(-YPRIME(1)-YPRIME(2))+P2+R24*(-Y(1)-Y(2))+RHCLIQ/2.*(Y(1)/FLUC0800
     1A45)**2*B1+RHOLIQ*Y(4)*G                                                 FLUC0810
      P3=P4-RHCLIC/.72*Y(2)*ABS(Y(2))/(A24-A45)**2                             FLUC0820
      CALL DVERK(N,FCN,X,Y,XEND,TOL,IND,C,NW,W,IER)                            FLUC0830
      IF(IND.LT.0.OR.IER.GT.0) GO TO 20                                        FLUC0840
      P6=P1/1000.                                                              FLUC0850
      POWER=Y(1)*(Y(1)/A45)**2*RHOLIC/2.                                       FLUC0860
      Y3=Y(3)-HE                                                               FLUC0870
      Y4=Y(4)-HE                                                               FLUC0880
      Y5=Y(5)-HE                                                               FLUC0890
      P7=P6-P5*.001                                                            FLUC0900
      V4=V-VE                                                                  FLUC0910
      WRITE(6,30) Y(1),POWER,Y3,Y4,Y5,X,P7,T2,V4                               FLUC0920
      T2=T2+DELT                                                               FLUC0930
      IF(T2.LT.TMAX) GO TO 10                                                  FLUC0940
      T2=TMAX                                                                  FLUC0950
10    CONTINUE                                                                 FLUC0960
      WRITE(6,87) TC,TH,R,D,F                                                  FLUC0970
      WRITE(6,88)                                                              FLUC0980
87    FORMAT(' TC=',F8.3,' TH=',F8.3,' R=',F10.3,' D=',E10.4,' F=',E10.4FLUC0990
     1)                                                                        FLU01000
88    FORMAT('  END OF PROGRAM')                                               FLU01010
64    CONTINUE                                                                 FLU01020
63    CONTINUE                                                                 FLU01030
62    CONTINUE                                                                 FLU01040
61    CONTINUE                                                                 FLU01050
60    CONTINUE                                                                 FLU01060
      STOP                                                                     FLU01070
50    FORMAT(12F6.0)                                                           FLU01080
51    FORMAT(6F6.0)                                                            FLU01090
52    FORMAT(I3)                                                               FLU01100
30    FORMAT(7E12.4,F7.1,'     ',E12.5)                                        FLU01110
35    FORMAT(' OUTPUT FLOW  OUTPUT POWER COLD DISPL  HOT DISPL OUTPUT DIFLUC1120
     1SPL       TIME  GAS PRESSURE HOT TEMP    GAS VOLUME')                  FLU01130
36    FORMAT('  (M3/S)          (WATTS)      (M)          (M)          (M) FLUC1140
     1          (S)       (KPA)      (K)          (M3) ')                   FLU01150
20    CONTINUE                                                                 FLU01160
      WRITE(6,40) IER,IND                                                      FLUC1170
40    FORMAT(2I3)                                                              FLU01180
      STOP                                                                     FLUC1190
      END                                                                      FLUC1200
      SUBROUTINE FCN(N,X,Y,YPRIME)                                             FLU01210
      DIMENSION Y(5),YPRIME(5)                                                 FLUC1220
      COMMON P4,P5,R45,RHOLIQ,G,A24,H45,P3,P1,R31,H13,A13,A45                  FLU01230
      IF((-Y(1)-Y(2)).GT.0.0) GO TO 11                                         FLU01240
      B2=1.0                                                                   FLUC1250
      GO TO 12                                                                 FLU01260
11    B2=0.0                                                                   FLU01270
12    CONTINUE                                                                 FLUC1280
      YPRIME(1)=(P4-P5-R45*Y(1)-Y(5)*RHOLIQ*G-RHOLIQ/2.*(-Y(1)-Y(2))**2/FLUC1290
     1A24/A24*B2)/H45                                                          FLUC1300
      YPRIME(2)=(P3-P1-R31*Y(2)-Y(3)*RHOLIQ*G)/H13                             FLUC1310
      YPRIME(3)=Y(2)/A13                                                       FLU01320
      YPRIME(4)=(-Y(1)-Y(2))/A24                                               FLU01330
      YPRIME(5)=Y(1)/A45                                                       FLUC1340
      RETURN                                                                   FLU01350
      END                                                                      FLUC1360
```

OUTPUT FLOW (M3/S)	OUTPUT POWER (WATTS)	COLD DISPL (M)	HOT DISPL (M)	OUTPUT DISPL (M)	TIME (S)	GAS PRESSURE (KPA)	HOT TEMP (K)	GAS VOLUME (M3)
-0.2320E-C9	-C.6245E-18	-0.1192E-06	0.5960E-07	-0.5960E-07	0.2500E-C1	-0.1221E-03	295.0	0.0
0.8480E-C6	C.3049E-07	-0.4172E-06	-0.2134E-04	0.1066E-03	0.5000E-01	0.6811E 00	299.0	0.14552E-10
0.2462E-05	C.7458E-C6	-C.1311E-05	-0.1050E-03	0.5200E-03	0.7500E-01	0.1302E 01	303.0	0.10652E-C7
0.4628E-C5	C.4956E-05	-0.4411E-05	-0.2829E-03	0.1407E-C2	0.1000E CC	0.1762E 01	307.0	0.52096E-07
0.7033E-C5	C.1739E-04	-C.1365E-04	-0.5713E-03	0.2865E-02	0.1250E 00	0.1978E 01	311.0	C.14079E-C6
C.9308E-C5	0.4032E-04	-0.3612E-C4	-0.9659E-C3	0.4908E-C2	0.1500E 00	0.1908E 01	315.0	0.28663E-06
0.1029E-C4	0.5446E-04	-0.8160E-04	-0.1421E-02	0.7359E-02	0.1750E 00	0.9059E 00	315.0	C.49098F-06
0.9764E-05	0.4654E-C4	-0.1616E-03	-0.1852E-C2	0.9866E-02	0.2000E CC	-0.2721E 00	315.0	0.73605E-06
0.7743E-05	0.2321E-04	-0.2872E-03	-0.2173E-C2	0.1205E-01	0.2250E CC	-0.1454E 01	315.0	0.98678E-06
0.4452E-C5	C.4412E-05	-0.4659E-03	-0.2306F-02	0.1358E-01	0.2500E 00	-0.2470E 01	315.0	C.12057E-C5
0.2940E-C6	0.1271E-C8	-C.6987E-03	-0.2194E-02	0.1417E-01	0.2750E CC	-0.3177E 01	315.0	0.13582F-C5
-0.4198E-C5	-C.3699E-05	-0.9783E-03	-0.1815E-02	0.1368E-01	0.3000E CC	-0.3470E C1	315.0	0.14175E-05
-0.8419E-C5	-C.2984E-04	-0.1287E-02	-0.1185E-C2	0.1210E-01	0.3250E 00	-0.3288E C1	315.0	0.13687E-C5
-0.1175E-04	-0.8118E-04	-0.1593E-02	-0.3639E-03	0.9582E-C2	0.3500E CC	-0.2620E C1	315.0	0.12109F-05
-0.1364E-C4	-C.1270E-03	-0.1855E-02	0.5466E-03	0.6406E-02	0.3750E CC	-0.1509E 01	315.0	0.95867E-06
-0.1367E-04	-0.1277E-03	-0.2030E-02	0.1419E-02	0.2991E-02	0.4000E 00	-0.5705E-01	315.0	0.64110E-06
-0.1162E-04	-0.7846E-04	-0.2082E-02	0.2116E-02	-0.1702E-03	0.4250E CC	0.1567E C1	315.0	0.29962E-06
-0.7592E-C5	-0.2188E-04	-0.1989E-02	0.2513E-02	-0.2572E-02	0.4500F CC	0.3132E C1	315.0	-C.16502E-C7
-0.2014E-C5	-C.4083E-06	-C.1749E-02	0.2517E-02	-0.3772E-C2	0.475CE CC	0.4373E C1	315.0	-0.25664E-C6
0.4359E-C5	0.4140E-05	-0.1373E-02	0.2081E-02	-0.3478E-C2	0.500CE CC	0.5033E 01	315.0	-0.37662E-06
0.1055E-C4	C.5866E-04	-0.8867E-03	0.1215F-02	-0.1614E-02	0.5250F CC	0.4934E 01	315.0	-0.34718E-C6
0.1553E-04	0.1873E-03	-0.3275E-03	-0.1013E-C4	0.1647E-C2	0.5500E CC	0.4038E C1	315.0	-0.16073E-06
0.1845E-C4	0.3142E-03	0.2543E-03	-0.1459E-02	0.5897E-02	0.5750E CC	0.2465E 01	315.0	0.16541F-C6
0.1880E-04	0.3320E-03	C.7995E-03	-0.2955E-C2	0.1055E-01	0.6000E CC	0.4662E 00	315.0	0.59037F-C6
0.1644E-04	0.2221E-03	0.1247E-02	-0.4302E-02	0.1496E-01	0.625CE CC	-0.1650E C1	315.0	0.10561E-05
0.1165E-C4	C.79C8E-04	0.1542E-02	-0.5313E-02	0.1847E-01	0.6500E CC	-0.3580E C1	315.0	0.14967F-C5
0.5011E-C5	C.6293E-05	0.1641E-02	-0.5838E-02	0.2055E-01	0.6750E CC	-0.5073E C1	315.0	0.18479E-05
-0.2677E-C5	-0.9590E-06	0.1521E-02	-0.5776E-02	0.2084E-01	0.7000E CC	-0.5946E 01	315.0	0.20561E-05
-0.1047E-C4	-C.5746E-04	0.1179E-02	-0.5099E-02	0.1920E-01	0.7250E CC	-0.6083E 01	315.0	0.20853E-C5
-0.1738E-04	-0.2623E-03	0.6483E-03	-0.3857E-C2	0.1572E-C1	0.7500E CC	-0.5428E 01	315.0	0.19207E-05
-0.2239E-C4	-C.5609E-03	-0.1490E-05	-0.2193E-02	0.1074E-01	0.7750E CC	-0.3987E C1	315.0	0.15725E-05
-0.2462E-C4	-0.7458E-C3	-0.6738E-03	-0.3213E-03	0.4867E-02	0.8000E CC	-0.1840E 01	315.0	0.10753E-C5
-0.2341E-C4	-0.6415E-03	-0.1270E-02	0.1500E-02	-0.1138E-02	0.825CE CC	0.8360E C0	315.0	0.48762E-06
-0.1850E-C4	-C.3168E-03	-0.1712E-02	0.3011E-C2	-0.6378E-02	0.8500E CC	0.3737E 01	315.0	-0.11281E-C6
-0.1020E-C4	-C.5312E-04	-0.1958E-02	0.3989E-C2	-0.9967E-02	0.875CE CC	0.6419E 01	315.0	-0.63676E-C6
0.4987E-C6	C.6201E-08	-0.1998E-02	0.4277E-02	-0.1118E-01	0.9000E CC	0.8345E 01	315.0	-0.99555E-C6
C.1198E-C4	C.8592E-04	-0.1841E-02	0.3801E-C2	-0.9617E-02	0.9250F CC	0.9017E 01	315.0	-0.11167E-05
0.2227E-C4	0.5522E-03	-0.1504E-02	0.2590E-02	-0.5334E-C2	0.9500E CC	0.8168E 01	315.0	-0.96057E-C6
0.2954E-04	0.1289E-02	-0.1026E-02	0.7902E-03	0.1145E-02	0.9750E CC	0.5891E 01	315.0	-0.53224E-C6
0.3256E-C4	0.1726E-02	-C.4706E-03	-0.135CE-C2	0.8911E-02	0.1000E 01	0.2616E 01	315.0	0.11570E-06
0.3087E-C4	0.1471E-02	0.8398E-04	-0.3523E-02	0.1684E-01	0.1025E 01	-0.1056E C1	315.0	0.89228E-06
0.2476E-C4	C.7589E-C3	0.5545E-03	-0.5413E-02	0.2380E-01	0.1050E C1	-0.4548E 01	315.0	0.16853F-C5
0.1508E-C4	C.1715E-C3	C.8664E-03	-0.6742E-02	0.2878E-01	0.1075E C1	-0.7417E 01	315.0	0.23808E-05
0.3030E-C5	0.1391E-05	0.9635E-03	-0.7301E-02	0.3104E-C1	0.1100E C1	-0.9372E 01	315.0	0.28788E-05
-0.1001E-C4	-C.5017E-04	0.8167E-03	-0.6975E-C2	0.3016E-01	0.1125E 01	-0.1024E 02	315.0	0.31051E-C5
-0.2254E-C4	-0.5728E-C3	0.4367E-03	-0.5764E-C2	0.2609E-C1	0.1150E C1	-0.9918E 01	315.0	0.30177E-05
-0.3300E-C4	-C.1796E-02	-0.9972E-04	-0.3811E-02	0.1915E-01	0.1175E C1	-0.8359E C1	315.0	0.26105F-05
-0.3981E-C4	-0.3154E-C2	-C.6489E-03	-0.1404E-02	0.1004E-01	0.1200E 01	-0.5559E 01	315.0	0.19160E-05
-0.4152E-04	-0.3580E-02	-0.1043E-02	0.1065E-02	-0.1264E-03	0.1225E 01	-C.1604E C1	315.0	C.10057E-C5
-0.3703E-C4	-0.2538E-02	-0.1146E-02	0.3173E-C2	-0.9947E-02	0.1250E 01	0.3252E C1	315.0	-0.11190E-C7

TC= 296.546 TH= 313.454 R= 286.847 D=0.6449E 01 F=0.7729E-01

END OF PROGRAM

DISTRIBUTION

DEFENSE DOCUMENTATION CENTER
CAMERON STATION, BUILDING 5
ALEXANDRIA, VA 22314
ATTN DDC-TCA (12 COPIES)

COMMANDER
USA RSCH & STD GPR (EUR)
BOX 65
FPO NEW YORK 09510
ATTN LTC JAMES M. KENNEDY, JR.
CHIEF, PHYSICS & MATH BRANCH

COMMANDER
US ARMY MATERIEL DEVELOPMENT &
READINESS COMMAND
5001 EISENHOWER AVENUE
ALEXANDRIA, VA 22333
ATTN DRXAM-TL, HQ TECH LIBRARY
ATTN DRCRD-TP, WILLIAM RALPH
ATTN DRCRD-TP, J. CORRIGAN

COMMANDER
USA ARMAMENT COMMAND
ROCK ISLAND, IL 61201
ATTN DRSAR-ASF, FUZE DIV
ATTN DRSAR-RDF, SYS DEV DIV - FUZES
ATTN DRSAR-RDG-T, MR. R. SPENCER
ATTN DRSAR-ASF
ATTN DRSAR-LEP-L, TECH LIBRARY

COMMANDER
USA MISSILE & MUNITIONS CENTER
& SCHOOL
REDSTONE ARSENAL, AL 35809
ATTN ATSK-CTD-F

COMMANDER IDDR&E
PENTAGON, ROOM 3D 1089
WASHINGTON, DC 20310
ATTN LTC G. KOPESAK

OFFICE OF THE DEPUTY CHIEF OF STAFF
FOR RES, DEV & ACQUISITION
DEPARTMENT OF THE ARMY
WASHINGTON, DC 20310
ATTN DAMA-ARP-P, DR. V. GARBER
ATTN MR. JOHN HILL, ROOM 3D424

US ARMY R&D GROUP (EUROPE)
BOX 15
FPO NEW YORK 09510
ATTN CHIEF, AERONAUTICS BRANCH
ATTN CHIEF, ENGINEERING SCIENCES

US ARMY RESEARCH OFFICE
P. O. BOX 12211
RESEARCH TRIANGLE PARK, NC 27709
ATTN JAMES J. MURRAY, ENG SCI DIV

COMMANDER
USA FOREIGN SCIENCE & TECH CENTER
FEDERAL OFFICE BUILDING
220 7TH STREET, NE
CHARLOTTESVILLE, VA 22901
ATTN DRXST-SD1

COMMANDER
USA MISSILE RES & DEV COMMAND
REDSTONE ARSENAL, AL 35809
ATTN REDSTONE SCIENTIFIC INFO
CENTER, DRSMI-RBD
ATTN DRDMI-TGC, WILLIAM GRIFFITH
ATTN DRDMI-TGC, JAMES G. WILLIAMS
ATTN DRDMI-TGC, J. C. DUNAWAY
ATTN DRCPM-TOE, FRED J. CHEPLEN

COMMANDER
USA MOBILITY EQUIPMENT R&D CENTER
FORT BELVOIR, VA 22060
ATTN TECH LIB (VAULT)
ATTN DRDME-EM, R. N. WARE

COMMANDER
EDGEWOOD ARSENAL
ABERDEEN PROVING GROUND, MD 21010
ATTN SAREA-MT-T, MR. D. PATTON

COMMANDER
US ARMY ARRADCOM
DOVER, NJ 07801
ATTN SARPA-TS-S-#59
ATTN DRDAR-LCN-F, A. E. SCHMIDLIN
ATTN DRDAR-LCW-E, MR. J. CONNOR
ATTN SARPA-ND-C-C, D. SAMPAR

COMMANDER
WATERVLIET ARSENAL
WATERVLIET ARSENAL, NY 12189
ATTN GARY W. WOODS
ATTN SARWV-RDT-L
ATTN JOHN BARRETT

COMMANDER
USA TANK AUTOMOTIVE RES & DEV CMD
ARMOR & COMP DIV, DRDTA-RKT
BLDG 215
WARREN, MI 48090
ATTN T. KOZOWYK
ATTN M. STEELE

COMMANDER
WHITE SANDS MISSILE RANGE
WHITE SANDS, NM 88002
ATTN STEWS-AD-L, TECH LIBRARY

COMMANDER
RODMAN LABORATORIES
ROCK ISLAND ARSENAL
ROCK ISLAND, IL 61201
ATTN SARRI-LA

OFFICE OF NAVAL RESEARCH
DEPARTMENT OF THE NAVY
ARLINGTON, VA 22217
ATTN STANLEY W. DOROFF, CODE 438
ATTN D. S. SIEGEL, CODE 211

DEPARTMENT OF THE NAVY
R&D PLANS DIVISION
ROOM 5D760, PENTAGON
WASHINGTON, DC 20350
ATTN BENJ R. PETRIE, JR., OP-987P4

COMMANDING OFFICER
NAVAL AIR ENGINEERING CENTER
LAKEHURST, NY 08733
ATTN ESSD, CODE 9314, HAROLD OTT

NAVAL AIR SYSTEMS COMMAND
DEPARTMENT OF THE NAVY
WASHINGTON, DC 20360
ATTN CODE AIR-52022A, J. BURNS
ATTN CODE AIR-52022E, D. HOUCK

COMMANDER
PACIFIC MISSILE RANGE
NAVAL MISSILE CENTER
POINT MUGU, CA 93042
ATTN CODE 3123, ABE J. GARRETT
ATTN CODE 1243, A. ANDERSON

COMMANDER
NAVAL SHIP ENGINEERING CENTER
PHILADELPHIA DIVISION
PHILADELPHIA, PA 19112
ATTN CODE 6772, D. KEYSER

COMMANDER
NAVAL SURFACE WEAPONS CENTER
WHITE OAK, MD 20910
ATTN CODE 413, CLAYTON MCKINDRA
ATTN CODE WA-33, J. O'STEEN
ATTN DIV 412, C. J. SEWELL

NAVAL POSTGRADUATE SCHOOL
MECHANICAL ENGINEERING
MONTEREY, CA 93940
ATTN CODE 69, PROF. R. NUNN

NAVAL SHIP RES & DEV CENTER
CODE 1619, MR. K. READER
BETHESDA, MD 20084

NAVAL SEA SYSTEMS COMMAND
SEA0331H
WASHINGTON, DC 20362
ATTN A. CHAIKIN

COMMANDER
NAVAL WEAPONS CENTER
CHINA LAKE, CA 93555
ATTN CODE 533, LIBRARY DIVISION
ATTN CODE 5536, MR. M. D. JACOBSON

COMMANDER
AF AERO PROPULSION LAB, AFSC
WRIGHT-PATTERSON AFB, OH 45433
ATTN LESTER SMALL 1TBC

COMMANDER
AIR FORCE AVIONICS LABORATORY
WRIGHT-PATTERSON AFB, OH 45433
ATTN RWN-2, RICHARD JACOBS

DIRECTOR
AF OFFICE OF SCIENTIFIC RESEARCH
1400 WILSON BLVD
ARLINGTON, VA 22209
ATTN NE, MR. G. KNAUSENBERGER

DISTRIBUTION (Cont'd)

DIRECTOR
APPLIED TECHNOLOGY LAB
FORT EUSTIS, VA 23504
ATTN DAVDL-EU-SYA, G. W. FOSDICK

COMMANDER
AF WEAPONS LABORATORY, AFSC
KIRTLAND AFB, NM 87117
ATTN SUL, TECHNICAL LIBRARY

COMMANDER
ARMAMENT DEV & TEST CENTER
EGLIN AIR FORCE BASE, FL 32542
ATTN ADTC (DLOSL), TECH LIBRARY

AIR FORCE FLIGHT TEST CENTER
6510 ABG/SSD
EDWARDS AFB, CA 93523
ATTN TECHNICAL LIBRARY

4950TH TEST WING (TZHM)
WRIGHT-PATTERSON AFB
DAYTON, OH 45424
ATTN MR. MICHAEL COLLINS

AF INSTITUTE OF TECHNOLOGY, AU
W RIGHT-PATTERSON AFB, OH 45433
ATTN LIBRARY AFIT(LD), BLDG 640, AREA B
ATTN AFIT(ENM), MILTON E. FRANKE (3 COPIES)

AEROSPACE MEDICAL DIVISION
BROOKS AFB, TX 78235
ATTN AMD/RDN, CPT G. JAMES

DIV OF REACTOR RES & DEV
F-309 US ERDA
WASHINGTON, DC 20545
ATTN FRANK C. LEGLER

OAK RIDGE NATIONAL LABORATORY
CENTRAL RES LIBRARY,
BLDG 4500N, RM 175
P. O. BOX X
OAK RIDGE, TN 37830
ATTN E. HOWARD

DEPARTMENT OF COMMERCE
BUREAU OF EAST-WEST TRADE
OFFICE OF EXPORT ADMINISTRATION
WASHINGTON, DC 20230
ATTN WALTER J. RUSNACK

SCIENTIFIC LIBRARY
US PATENT OFFICE
WASHINGTON, DC 20231
ATTN MRS. CURETON

DEPARTMENT OF COMMERCE
NATIONAL BUREAU OF STANDARDS
WASHINGTON, DC 20234
ATTN GUSTAVE SHAPIRO, 425.00

NASA AMES RESEACH CENTER
MOFFETT FIELD, CA 94035
ATTN MS 244-13, DEAN CHISEL

COMMANDER
NAVAL AIR DEVELOPMENT CENTER
WARMINSTER, PA 18974
ATTN R. MCGIBONEY, 30424
ATTN CODE 8134, LOIS GUISE

NASA LEWIS RESEARCH CENTER
21000 BROOKPARK ROAD
CLEVELAND, OH 44135
ATTN VERNON D. GEBBEN

NASA SCIENTIFIC & TECH INFO FACILITY
P. O. BOX 8657
BALTIMORE/WASHINGTON
INTERNATIONAL AIRPORT, MD 21240
ATTN ACQUISITIONS BRANCH

UNIVERSITY OF ALABAMA
CIVIL & MINERAL ENGINEERING DEPT.
P. O. BOX 1468
UNIVERSITY, AL 35486
ATTN DR. HAROLD R. HENRY

ARIZONA STATE UNIVERSITY
ENGINEERING CENTER
TEMPE, AZ 85281
ATTN PETER K. STEIN, LABORATORY FOR MEASUREMENT SYS ENGR

UNIVERSITY OF ARKANSAS
TECHNOLOGY CAMPUS
P. O. BOX 3017
LITTLE ROCK, AR 72203
ATTN PAUL C. MCLEOD

UNIVERSITY OF ARKANSAS
MECHANICAL ENGINEERING
FAYETTEVILLE, AR 72701
ATTN JACK H. COLE, ASSOC PROF

CARNEGIE-MELLON UNIVERSITY
SCHENLEY PARK
PITTSBURGH, PA 15213
ATTN PROF W. T. ROULEAU, MECH ENGR DEPT

CASE WESTERN RESERVE UNIVERSITY
UNIVERSITY CIRCLE
CLEVELAND, OH 44106
ATTN PROF P. A. ORNER

THE CITY COLLEGE OF THE CITY
UNIVERSITY OF NEW YORK
DEPT OF MECH ENGR
139TH ST. AT CONVENT AVENUE
NEW YORK, NY 10031
ATTN PROF L. JIJI
ATTN PROF G. LOWEN

DUKE UNIVERSITY
COLLEGE OF ENGINEERING
DURHAM, NC 27706
ATTN C. M. HARMAN

ENGINEERING SOCIETIES LIBRARY
345 EAST 47TH STREET
NEW YORK, NY 10017

COMMANDER
AIR FORCE FLIGHT DYNAMICS LAB
WRIGHT-PATTERSON AFB, OH 45433
ATTN AFFDL/FGL, H. SNOWBALL

IIT RESEARCH INSTITUTE
10 WEST 35TH STREET
CHICAGO, IL 60616
ATTN DR. K. E. MCKEE

LEHIGH UNIVERSITY
DEPT. OF MECHANICAL ENGINEERING
BETHLEHEM, PA 18015
ATTN PROF FORBES T. BROWN

LINDA HALL LIBRARY
5109 CHERRY STREET
KANSAS CITY, MO 64110
ATTN DOCUMENTS DIVISION

MASSACHUSETTS INSTITUTE OF TECHNOLOGY
77 MASSACHUSETTS AVENUE
CAMBRIDGE, MA 02139
ATTN ENGINEERING TECHNICAL REPORTS, RM 10-408
ATTN DAVID WORMLEY, MECH ENGR DEPT, RM 3-146

MICHIGAN TECHNOLOGICAL UNIVERSITY
LIBRARY, DOCUMENTS DIVISION
HOUGHTON, MI 49931
ATTN J. HAWTHORNE

UNIVERSITY OF MISSISSIPPI
201 CARRIER HALL, DEPT OF MECH ENGR
UNIVERSITY, MS 38677
ATTN DR. JOHN A. FOX

MISSISSIPPI STATE UNIVERSITY
DRAWER ME
STATE COLLEGE, MS 39672
ATTN DR. C. J. BELL, MECH ENG DEPT

UNIVERSITY OF NEBRASKA LIBRARIES
ACQUISITIONS DEPT, SERIALS SECTION
LINCOLN, NE 68508
ATTN ALAN GOULD

UNIVERSITY OF NEW HAMPSHIRE
MECH ENGR DEPT, KINGSBURY HALL
DURHAM, NH 03824
ATTN PROF CHARLES TATE (3 COPIES)

DEPT OF MECHANICAL ENGINEERING
NEWARK COLLEGE OF ENGINEERING
323 HIGH STREET
NEWARK, NJ 07102
ATTN DR. R. A. COMPARIN
ATTN DR. R. Y. CHEN

NASA LANGLEY RESEARCH CENTER
HAMPTON, VA 23665
ATTN MS 494, H. D. GARNER
ATTN MS 494, R. R. HELLBAUM
ATTN MS 185, TECHNICAL LIBRARY

DISTRIBUTION (Cont'd)

OHIO STATE UNIVERSITY LIBRARIES
SERIAL DIVISION, MAIN LIBRARY
1858 NEIL AVENUE
COLUMBUS, OH 43210

OKLAHOMA STATE UNIVERSITY
SCHOOL OF MECH & AEROSPACE ENGR.
STILLWATER, OK 74074
ATTN PROF. KARL N. REID

PENNSYLVANIA STATE UNIVERSITY
215 MECHANICAL ENGINEERING BUILDING
UNIVERSITY PARK, PA 16802
ATTN DR. J. L. SHEARER

FRANKLIN INSTITUTE OF THE STATE OF PENNSYLVANIA
20TH STREET & PARKWAY
PHILADELPHIA, PA 19103
ATTN KA-CHEUNG TSUI, ELEC ENGR DIV
ATTN C. A. BELSTERLING

PENNSYLVANIA STATE UNIVERSITY
ENGINEERING LIBRARY
201 HAMMOND BLDG
UNIVERSITY PARK, PA 16802
ATTN M. BENNETT, ENGINEERING LIBRARIAN

PURDUE UNIVERSITY
SCHOOL OF MECHANICAL ENGINEERING
LAFAYETTE, IN 47907
ATTN PROF. VICTOR W. GOLDSCHMIDT
ATTN PROF. ALAN T. MCDONALD

ROCK VALLEY COLLEGE
3301 NORTH MULFORD ROAD
ROCKFORD, IL 61101
ATTN KEN BARTON

RUTGERS UNIVERSITY
LIBRARY OF SCIENCE & MEDICINE
NEW BRUNSWICK, NJ 08903
ATTN GOVERNMENT DOCUMENTS DEPARTMENT,
MS. SANDRA R. LIVINGSTON

SYRACUSE UNIVERSITY
DEPARTMENT OF MECHANICAL & AEROSPACE ENGINEERING
139 E. A. LINK HALL
SYRACUSE, NY 13210
ATTN PROF. D. S. DOSANJH

UNIVERSITY OF TEXAS AT AUSTIN
DEPARTMENT OF MECHANICAL ENGINEERING
AUSTIN, TX 78712
ATTN DR. A. J. HEALEY

TULANE UNIVERSITY
DEPARTMENT OF MECHANICAL ENGINEERING
NEW ORLEANS, LA 70118
ATTN H. F. HRUBECKY

UNION COLLEGE
MECHANICAL ENGINEERING
SCHENECTADY, NY 12308
ATTN ASSOCIATE PROFESSOR W. C. AUBREY, MECHANICAL
ENGINEERING DEPARTMENT, STEINMETZ HALL

VIRGINIA POLYTECHNIC INSTITUTE & STATE UNIVERSITY
MECHANICAL ENGINEERING DEPARTMENT
BLACKSBURG, VA 24061
ATTN PROF. H. MOSES

WASHINGTON UNIVERSITY
SCHOOL OF ENGINEERING
P. O. BOX 1185
ST. LOUIS, MO 63130
ATTN W. M. SWANSON

WEST VIRGINIA UNIVERSITY
MECHANICAL ENGINEERING DEPARTMENT
MORGANTOWN, WV 26505
ATTN DR. RICHARD A. BAJURA

WICHITA STATE UNIVERSITY
WICHITA, KS 67208
ATTN DEPT AERO ENGR, E. J. RODGERS

UNIVERSITY OF WISCONSIN
MECHANICAL ENGINEERING DEPARTMENT
1513 UNIVERSITY AVENUE
MADISON, WI 53706
ATTN FEDERAL REPORTS CENTER
ATTN NORMAN H. BEACHLEY, DIR, DESIGN ENGINEERING LAB

WORCESTER POLYTECHNIC INSTITUTE
WORCESTER, MA 01609
ATTN GEORGE C. GORDON LIBRARY (TR)
ATTN TECHNICAL REPORTS

US ARMY ELECTRONICS RESEARCH & DEVELOPMENT COMMAND
ATTN WISEMAN, ROBERT S., DR., DRDEL-CT
ATTN PAO
ATTN MANION, F., DRDEL-AP-CCM

HARRY DIAMOND LABORATORIES
ATTN 00100, COMMANDER/TECHNICAL DIR/TSO
ATTN CHIEF, 00210
ATTN CHIEF, DIV 10000
ATTN CHIEF, DIV 20000
ATTN CHIEF, DIV 30000
ATTN CHIEF, DIV 40000
ATTN CHIEF, LAB 11000
ATTN CHIEF, LAB 13000
ATTN CHIEF, LAB 15000
ATTN CHIEF, LAB 21000
ATTN CHIEF, LAB 22000
ATTN CHIEF, LAB 34000
ATTN CHIEF, LAB 36000
ATTN CHIEF, LAB 47000
ATTN CHIEF, LAB 48000
ATTN RECORD COPY, 94100
ATTN HDL LIBRARY, 41000 (5 COPIES)
ATTN HDL LIBRARY (WOODBRIDGE)
ATTN CHAIRMAN, EDITORIAL COMMITTEE
ATTN TECHNICAL REPORTS BRANCH, 41300
ATTN LEGAL OFFICE, 97000
ATTN LANHAM, C., 00210
ATTN WILLIS, B., 47400
ATTN CHIEF, BRANCH 13300
ATTN CHIEF, BRANCH 13400 (10 COPIES)
ATTN DRZEWIECKI, T., 13400 (10 COPIES)